Characterization of the Main Frequency Shifts for the Brazilian ^{133}Cs Atomic Beam Frequency Standard

A. Bebeachibuli, M. S. Santos, D. V. Magalhães, S. T. Müller, and V.S. Bagnato
Instituto de Física de São Carlos – USP
Caixa Postal 369, CEP 13560-970, São Carlos/SP, Brazil

Received on 8 August, 2005

In order to evaluate an atomic clock, it is important to determine the main frequency shifts caused by external fields, device imperfections, etc. Scanning the frequency of the main oscillator, the Ramsey fringe is obtained and used to determine the main shifts. The gravitational shift (10^{-17}), second order Doppler (1.65×10^{-13}), Black-Body radiation shift (2.9×10^{-14}), quadratic Zeeman effect (5×10^{-13}), Rabi Pulling (1.3×10^{-13}) and cavity pulling (1.3×10^{-13}) have been evaluated. The short term stability, $(6.6\pm0,2)\times10^{-13}$, was obtained.

I. INTRODUCTION

An atomic frequency standard is a device that generates an output signal which derives from an inherent property of an atom, like its constant resonant frequency in time. This property confers on the output signal several characteristics such as high accuracy, great stability and reproducibility with time [1,2]. In this approach, the principle of operation of an atomic frequency standard is the frequency stabilization with respect to a local oscillator, operating in a frequency corresponding to an atomic transition between two well known energy levels. In 1967, the SI second was defined as "the duration of 9 192 631 770 periods of the radiation corresponding to the transition between the two hyperfine levels of the ground state of the caesium 133 atom". The reference atomic transition is, in spectroscopy notation, $6S_{1/2}\,|F=3,m_F=0\rangle \longleftrightarrow 6S_{1/2}\,|F=4,m_F=0\rangle$. This definition refers to a caesium atom at rest at a temperature of 0K. This transition can be accessed in the following way: the Cs atoms are prepared in the state F=3 and interact with two microwave fields spacially separated by a region free of oscillatory radiation. This is known as the method of successive oscillatory fields, named as Ramsey interrogation method [3]. In the optimum condition of power and frequency of the microwave field inside the interrogation cavity, the transition probability between the state $|F=3,m_F=0\rangle \longleftrightarrow |F=4,m_F=0\rangle$ is maximized. Finally, the atomic transition rate as a function of frequency is measured. The resonance peak is observed around $\nu_0\,(1+\varepsilon)$, where ε corresponds to the frequency shift due to many external perturbations.

The aim of this paper is the description and the characterization of the atomic standard fully constructed in Brazil [4]. We report the major shifts present in our atomic frequency standard, like the Quadratic Zeeman, Cavity Pulling and Rabi Pulling. The performance of the standard can be summarized in a global uncertainty table and the determined short-term stability.

II. DESCRIPTION OF THE FREQUENCY STANDARD DEVICE

The Brazilian ^{133}Cs atomic beam frequency standard has been well described elsewhere [4]. The vaccum system is enclosed in a cylindrical chamber made of stainless steel; it is 60 cm long and its diameter is 20 cm. The background pressure in the chamber is lower than 10^{-5} Pa and it is maintained with a turbo molecular pump. An effusive oven heated to about 343K produces the ^{133}Cs atomic beam axial to the system. An array of stainless steel and graphite disks collimates the beam to less than 2 x 10^{-4} sr. The produced C-field is perpendicular to the atomic beam and his magnitude is about 20 μT. Before getting into the microwave cavity, the atoms are optically prepared in the $6^2S_{1/2}$(F = 3) ground level with a laser beam resonant with the transition $6^2S_{1/2}$ (F = 4) $\rightarrow$ $6^2P_{3/2}$(F'= 4). After passing through both microwave zones, the fluorescence of the atoms that interact with a laser beam resonant with the transition $6^2S_{1/2}$ (F = 4) $\rightarrow$ $6^2P_{3/2}$(F'= 5) is detected. The optical pumping and the detection beams are produced by a single mode diode laser (SDL 5410C - 852nm), stabilized in an extended cavity configuration. The linewidth of the laser is estimated to be less than 500 kHz. The saturated absorption spectroscopy technique is used to lock the laser in the $6^2S_{1/2}$ (F = 4)$\rightarrow$$6^2P_{3/2}$ (F'= 5) transition. The optical pumping beam is generated by an acousto-optical modulator operating at 251 MHz.

The microwave cavity has a conventional U shape. It is made of copper and the distance between the interrogation zones is 10 cm. The quality factor (Q) of the cavity is about 500. The microwave synthesizer was built by F. Walls and co-workers at NIST (Boulder - USA) and it generates the 9.192631770 GHz from three quartz oscillators at 5 MHz, 100 MHz and 10.7 MHz. The modulation of the 9.192 GHz signal is injected in the 10.7 MHz oscillator by an external DDS (Stanford DS 345). A LabVIEW^{TM} computer interface program implemented by our group performs the control of the standard. The evaluation of the Caesium beam frequency standard performance has been made by comparison with a commercial standard (Agilent 5071-A).

Many changes have been performed in the system in order to optimize its performance with respect to the previous eval-

uation [4]. The optimum microwave power was determined to increase the output signal of the atomic frequency standard, assuring that the atoms suffer a $\pi/2$ pulse in each interrogation cavity. The static magnetic field inhomogeneity, generated by the C-field, has been minimized improving its current supply.

A new temperature control for the oven was also implemented. To heat it, two heatbelt are used, one in the colimation region and other on the Cs resevoir. Doing so, the operation temperature of the oven and consequently the velocity distribution of the beam could be reduced. The oven temperature was adjusted so that the signal obtained with the standard is high enough, without being saturated, and the signal to noise ratio was preserved.

The Ramsey fringe, which is the characteristic signature of an atomic frequency standard, obtained in this new configuration is shown in Fig. 1, where a good symmetry and signal to noise ratio are observed.

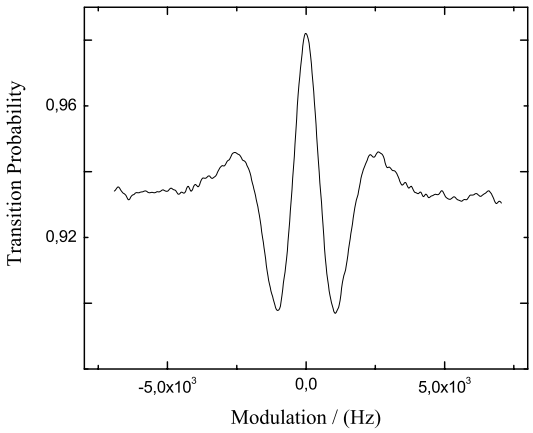

FIG. 1: The clock transition, $|3,0\rangle \leftrightarrow |4,0\rangle$, measured with the Brazilian ^{133}Cs atomic beam standard.

III. FREQUENCY SHIFTS

A. Gravitacional Frequency Shift

This shift is a relativistic correction due to the gravitational potential variation of the standard position at a given location. It is independent of the atomic velocity and just produces a translation at the Ramsey fringe. For standard on the Earth, or close to its surface, the effect of the gravitational potential is taken on the geoid surface [5]. The frequency of an atomic standard is shifted by an amount $\Delta\nu_G$, when it is fixed in an altitude h above the geoid by

$$\frac{\Delta\nu_G}{\nu_0} = -\frac{g}{c^2}h \tag{1}$$

where g is the gravitational acceleration (according to the 3^{rd} Conférence Génerale des Poids et Mesures, CGPM, in 1901, its value is 980.655 cm/s^2) and c is the light speed (299,792,498 km/s, defined in the 15^{th} CGPM, in 1975). The São Carlos altitude where the atomic beam standard is located, is $h = (850 \pm 50)\,m$. This was measured with a GPS receiver (9390 - 6000 Datum). Following, the frequency shift due to the gravitational shift is $\frac{\Delta\nu_G}{\nu_0} = -1.0 \times 10^{-17}$.

B. Second-order Doppler shift

The second-order Doppler shift is related to the temporal dilatation predicted in special relativity. Each velocity component in the beam adds a shift given by

$$\frac{\Delta\nu_G}{\nu_0} = -\frac{\upsilon^2}{2c^2} \tag{2}$$

where c is the light speed and v is the atomic speed computed for a time of flight τ. We have used the method described in [6], which uses a mathematical procedure to extract from the Ramsey pattern some characteristic parameters without having to determine the time of flight distribution of the atoms. In the limit where $a\tau\Delta \ll 1$ (a is the ratio between L, the lenght between the two interrogation zones of the microwave cavity, and l, the lenght of the interaction region), the correction in the resonance frequency is given by

$$\nu_D = -\frac{\nu_0 l^2}{2c^2}\frac{\int \frac{1}{\tau^2}A(\nu_m,b,\tau)\,f(\tau)\,d\tau}{\int A(\nu_m,b,\tau)\,f(\tau)\,d\tau} \tag{3}$$

In equation 3, the function $A(\nu_m,b,\tau)$ and $f(\tau)$ represent respectively the unperturbed transition probability, (function of the modulation amplitude, ν_m, the Rabi frequency b and τ) and the time of flight distribution given by the Maxwell speed distribution.

Figure 2 shows the dependence of the second-order Doppler shift as a function of the modulation amplitude on the microwave signal for normal operation of the standard. For the given oven temperature ($T = 343K$), the average atomic speed is (200 ± 7) m/s. A typical modulation in the Ramsey fringe is 45 Hz, so that the resulted shift is $\frac{\nu_D}{\nu_0} = -1.65 \times 10^{-13}$.

C. Black Body radiation shift

The presence of a small perturbation created by a non-resonant oscillatory electrical field, due to black body radiation at the cavity temperature T, introduces a shift on the atomic energy levels [7]. The shift is significant in primary Cs atomic beam frequency standards and is calcuated to be [8]

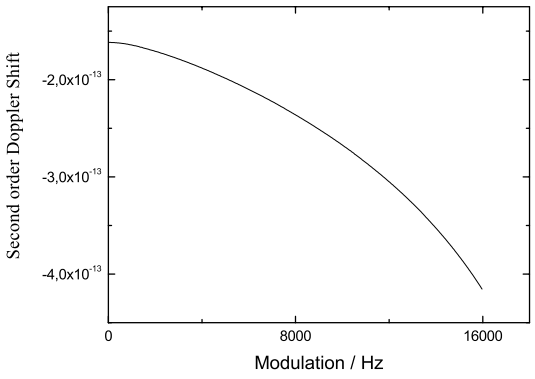

FIG. 2: Dependence of the second-order Doppler shift as a function of the modulation amplitude for a temperature oven of 343 K and an average speed 200 m/s.

$$\frac{\Delta\nu_T}{\nu_0} = -K^{"}\left(\frac{T}{300}\right)^4\left[1+\varepsilon\left(\frac{T}{300}\right)^2\right] \quad (4)$$

$$= -1.69\times10^{-14}\left(\frac{T}{300}\right)^4 \quad (5)$$

where K" = 1.573(3)$\times10^{-14}$ Hz and ε =1.4$\times10^{-2}$ [9]. The operational temperature is measured with a calibrated thermistor and for the present report $T = (343\pm2)$ K, resulting in a black body radiation shift of $\frac{\Delta\nu_T}{\nu_0} = -(2.887\pm0.04)\times10^{-14}$.

D. Quadratic Zeeman effect

In an atomic frequency standard, which is based on the transition between two specific hyperfine sublevels, it becomes important to work with the presence of a dc magnetic field (C-field). This field lifts the degeneracy of the manyfold levels, and therefore the atomic transition line depends C-field amplitude.

We have minimized the field inhomogeneity and improved the C-field control. After these improvements, the second-order Zeeman shift was evaluated. For this, we have applied the method described by Makdissi et al [6], where a periodic measurement of the Zeeman frequency between a pair of transitions with the same absolute value of magnetic quantum number is performed. We have chosen the $6^2S_{1/2}$(F = 3, m_F = 1) $\rightarrow$ $6^2S_{1/2}$(F = 4, m_F = 1) and $6^2S_{1/2}$(F = 3, m_F = -1) $\rightarrow$$6^2S_{1/2}$(F = 4, m_F = -1) transitions. The transition frequency between these two levels of the ground state with Δm_F = 0 is given by:

$$\nu_m = \nu_0\sqrt{1+(m/2)x+x^2} \quad (6)$$

where $x \approx 3.0496B_0$, B_0 is the magnitude of the C-field (20μT) and ν_0 is the atomic resonant frequency in the absence of magnetic field. The average value of x is small for the usual values of B_0 so that it is possible to expand equation 6 in power series and the resonant frequency for the transitions in which $m_F \neq 0$ is given by:

$$\nu_m = \nu_0[1+(m/4)\langle x\rangle + (1/2)\left(1-m^2/16\right)\langle x^2\rangle \quad (7)$$

where $\langle\rangle$ represents an average over the free of oscillating field region, of lenght L. In practice, we measure $\langle x\rangle$ instead of $\langle B_0\rangle$ to avoid any uncertainty between the constant that relates the two variables. The value of $\langle x\rangle$ is obtained from the resonant frequency of ν_1 and ν_{-1}, resulting in

$$\langle x\rangle = (4/\nu_0)\left[(\nu_1-\nu_{-1})/2\right] = 4f_z/\nu_0 \quad (8)$$

where the quantity f_z is the Zeeman frequency. Because the field has almost constant amplitude B_0 along the atoms trajectory, we can make the approximation $\langle x^2\rangle = \langle x\rangle^2$, so that we can express the second order Zeeman shift as:

$$\nu_Z = 8f_z^2/\nu_0 \quad (9)$$

In our atomic frequency standard we have f_z = 92 kHz and the second order Zeeman shift is about 7.3 Hz.

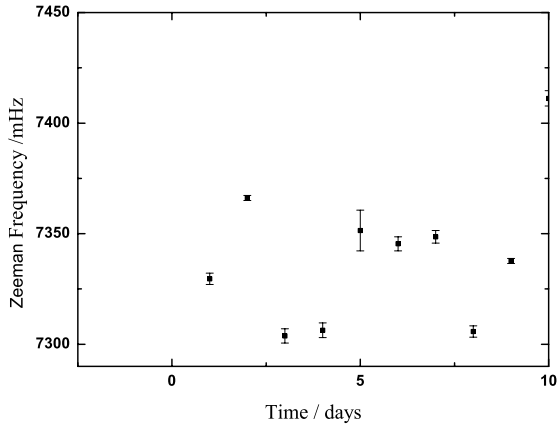

FIG. 3: Time variation of the quadratic Zeeman shift.

A periodic measurement of the ν_{-1} and ν_{+1} Zeeman frequency is necessary to observe its temporal dependence. We have measured it for ten days, five times per day, to study the way it changes in normal operating condition in the laboratory. Fig. 3 shows the obtained variations of the quadratic Zeeman shift. The uncertainty in the measure of the frequency transitions, ν_{-1} and ν_{+1}, is imposed by the stability of the atomic beam standard. Using the equation 9 it is possible to write

$$\frac{\delta\nu_Z}{\nu_0} = 2\frac{\nu_Z}{\nu_0}\frac{\delta f_Z}{f_0} \quad (10)$$

resulting in an uncertainty of 1.5×10^{-14} for $\delta f_Z = 0.8$ Hz.

From Fig. 3, it is possible to see that the daily variation of ν_Z is of about $5\times10^{-3}Hz$. Therefore, the relative uncertainty in the temporal measurement of the quadratic Zeeman shift is $\Delta\nu/\nu_0 = 5.43\times10^{-13}$.

E. Inhomogeneity of the magnetic field along the microwave cavity

The resonant line shape of a thermal beam is a superposition of a narrow spectral feature (Ramsey fringe) on a broader resonance (Rabi pedestal). In ideal conditions, the Ramsey fringe is centered within the Rabi pedestal. If there is any inhomogeneity in the magnetic field along the atom trajectory through the microwave cavity, a frequency shift in the resonant line is observed and the Ramsey fringe is not anymore centered in the Rabi pedestal [7].

The centers of the Rabi line and of the Ramsey line have been measured for each of the neighbour transitions ($\Delta m_F = 0$) and for the clock transition. The difference between them was computed and it can be written as [7]:

$$D(m) = \nu^{Ram}(m) - \nu^{Rabi}(m) = \nu_0(m/8)(\varepsilon_1+\varepsilon_2) \qquad (11)$$

where ε_1 and ε_2 are fluctuations of the mean static field in the first and second interaction regions respectively. The slope in the linear curve of $D(m)$ as a function of m determines the value $(\varepsilon_1+\varepsilon_2)$.

The modulation of the 9.192 GHz signal, introduced in the 10.7 MHz oscillator of the microwave synthesizer, has been driven by a computer program that makes possible to choose the modulation amplitude and lock the system to the center of the Ramsey line or to the center of the Rabi line for each neighbour transition and for the clock transition. We have compared the output signal of the 5 MHz oscillator with the 5 MHz output signal from the commercial Cs standard. A computer program collects these oscillation data during fifty minutes per line. Fig. 4 shows the measured shifts for all $\Delta m_F = 0$ transitions.

The estimated linear slope from the experimental curve $D(m)\times m_F$ is (11.35 ± 0.05) resulting in $(\varepsilon_1+\varepsilon_2) = -(0.99\pm0.05)\times10^{-8}$. For the operating condition of the standard, the frequency error on the clock transition due to the field inhomogeneity is $\nu_Z = (1.08\pm0.04)\times10^{-5}Hz$.

The other Zeeman transitions are also shifted by the same effect and it is necessary to count them. As the velocity distribution is the same for all transitions, we have used the same procedure to study the effect of the magnetic inhomogeneity for the $m_F \neq 0$ transition. The Zeeman frequency is shifted by an amount $f_z = 0.77\mu Hz$ and this is equivalent to a residual error of $\frac{\Delta\nu_Z}{\nu_0} \leq 8.3\times10^{-15}$.

Finally, the total uncertainty is computed considering the uncertainty measured due the experimental determination of the Zeeman frequency $\frac{\Delta\nu_Z}{\nu_0} = 5.43\times10^{-13}$ and the correction due the field inhomogeneity, $\frac{\Delta\nu_Z}{\nu_0} = 0.08\times10^{-13}$. The quadratic sum of this terms results in $\frac{\Delta\nu_Z}{\nu_0} = 5.5\times10^{-13}$, with an uncertainty of 0.15×10^{-13}.

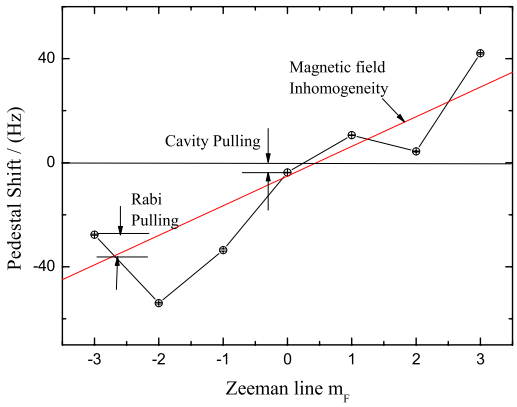

FIG. 4: Frequency difference $D(m)$ between the center of the Ramsey fringe and the Rabi pedestal as a function of the Zeeman sublevels number m_F. The points deviate from the straight line because of the Rabi Pulling effect. The applied C-field is $B_0 = 20\mu T$.

F. Rabi Pulling

Besides the clock transition, there are other six transitions linearly dependent of the static magnetic field, $\Delta F = \pm1, \Delta m_F = 0$, as shown in Fig. 5.

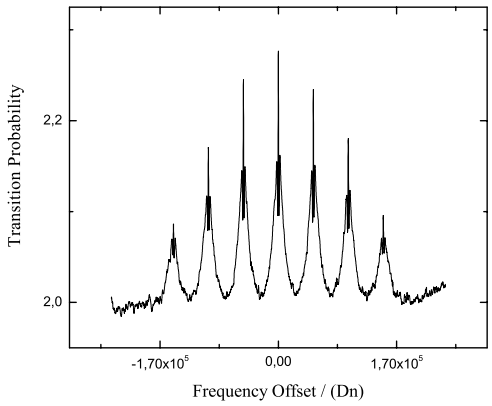

FIG. 5: The Zeeman spectrum of the ^{133}Cs atom obtained with the atomic beam frequency standard.

Their amplitudes are comparable to the clock transition and consequently they shift the defined frequency transition. The Rabi Pulling results from the overlapping wings of adjacent transitions in the Zeeman spectrum. The pedestals of the transitions $(F=4,m_F=1) \longleftrightarrow (F=3,m_F=1)$ and $(F=4,m_F=-1) \longleftrightarrow (F=3,m_F=-1)$ overlap the pedestal of the clock transition $(F=4,m_F=0) \longleftrightarrow (F=3,m_F=0)$ so that the resolution between the resonant

line is not clear and a frequency shift is added to the detected atoms which are directly related to the transition.

The clock transition is shifted by the Rabi Pulling only if there is an asymmetry between the transitions $m_F = 1$ and $m_F = -1$. From Fig. 5, we observe that there is an asymmetry of 1,3% in the peacks high of these transitions. If we assume that 1,3% is the worst asymmetry achieved with this value of C-field, it is possible to estimate the fractional Rabi Pulling as 4.4×10^{-11}. The corresponding pulling for the Ramsey fringe is smaller by a quantity of $\left(\frac{l}{2L}\right)$, where l is the interrogation cavity length, and its magnitude is 1.3×10^{-13}. As observed, the Rabi pulling for the Rabi pedestal is larger than for the Ramsey fringe because the pedestal slope is smaller and the modulation amplitude is larger.

To determine the Rabi Pulling, a similar procedure to obtain the field inhomogeneity was used. The shift between the pedestal and its corresponding fringe for each transition was measured. The C-field has been adjusted for $B_0 = 20$ μT and $B_0 = 30$ μT. The results are depicted in Figs. 4 and 6. It is possible to observe, for the $m_F = \pm 2$ transitions, a shift between the Rabi pedestal and the Ramsey Fringe of about 33 Hz and 2.46 Hz for $B_0 = 20$ μT and $B_0 = 30$ μT, respectively. They correspond to a Rabi Pulling of about 1.67×10^{-11} and 7.13×10^{-12} for the Rabi pedestal when $B_0 = 20$ μT and $B_0 = 30$ μT. For the Ramsey fringes the pullings are 4.75×10^{-14} and 2.07×10^{-14}, on the same values of B_0.

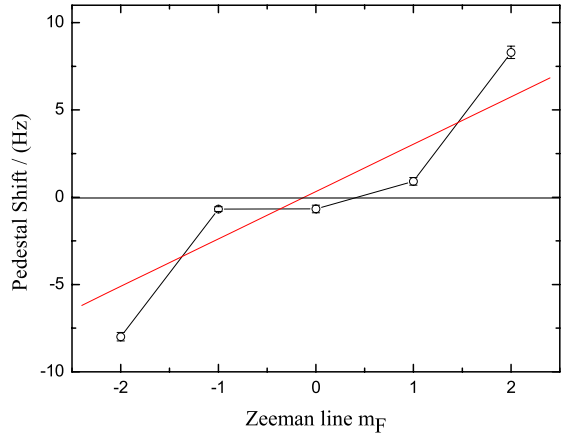

FIG. 6: Frequency difference $D(m)$ between the center of the Ramsey fringe and the center of the Rabi pedestal as a function of the Zeeman sublevels number m_F, for a higher magnetic field compared to Fig. 4. The applied C-field is $B_0 = 30\mu T$. The points are much closer to the straight line because the Rabi Pulling is less important.

G. Cavity Pulling

The cavity pulling arises from the variation of the microwave amplitude with the frequency when the cavity is mistunned. It is nearly independent of m_F, but it has a strong dependence on the microwave power and on the modulation amplitude. Consequently, the Cavity Pulling is larger for the Rabi pedestal than for the Ramsey fringe.

Our procedure to measure the cavity pulling has been similar to that described by Shirley et al [8] and it is again the same used to measure the magnetic field inhomogeneity. Since the cavity pulling is nearly independent of m_F and the Rabi pulling for the clock transition is small [8,10], the pedestal shift shown in Fig. 4 corresponds to the cavity pulling. The measured pedestal shift is (3.76 ± 0.10) Hz for a measurement time of 1000 s and the induced effect on the Ramsey fringe for the cavity detunning is 1.27×10^{-13}.

H. Global Accuracy Budget

The accuracy of an atomic frequency standard is defined as the capacity of the standard to produce a frequency that is in agreement with the definition of the second. It is expressed like a relative uncertainty $\left(\frac{\Delta\nu}{\nu_0}\right)$ relative to the second definition. Applying the several corrections to our frequency standard, and their corresponding uncertainty, table I was constructed, with each uncertainty obtained earlier being described.

Freq. Shift	Corr.($\times 10^{-13}$)	Uncer.($\times 10^{-13}$)
Red Shift	-1$\times 10^{-4}$	5$\times 10^{-5}$
2nd order Doppler	-1.65	0.12
Quadratic Zeeman	5.5	0.15
Cavity Pulling	1.27	0.09
Rabi Pulling	1.3	0.05
Black Body Rad.	-0.2887	0.004

TABLE I: Uncertainty table of the atomic beam clock

Finally, the global accuracy of the beam standard is $\sigma_C = 6.13 \times 10^{-13}$. This value means the precision in which our frequency standard measures the clock transition frequency around 9.192.631.770 Hz.

I. Stability

The stability of an atomic frequency standard caracterizes the capacity of a standard to reproduce the same average frequency along the time. It is determined by the square root of the Allan variance

$$\sigma_y(\tau) = \frac{1}{\pi} \frac{1}{Q_{at}(S/N)} \sqrt{\frac{t}{\tau}} \tag{12}$$

where τ is the sampling time, Q_{at} is the quality factor of the atomic resonance, S/N is the signal to noise ratio for a sampling time τ and t is the cycle time.

The short-term stability has been measured using a commercial atomic standard (Agilent - 5071A) and a computer with a GPIB interface to store the data reading, allowing us

to perform a constant performance evaluation of the atomic beam standard. Fig. 7 shows the short-term stability obtained with our ^{133}Cs beam frequency standard versus the sampling time τ. For comparison we have include in Fig. 7 the stability of the same standard in 1998 (the first evaluation), $\sigma_y(\tau) = (1.2 \pm 0.7) \times 10^{-9}\tau^{-0,56\pm0.7}$. This poor stability was attributed to several factors, like mechanical and thermal noise in the clock room and a limited signal to noise ratio in the atomic detection. Several changes were performed, including the construction of a room free of mechanical vibrations and thermally isolated. These changes increased the laser stability and, consequently, the signal to noise ratio. For the present evaluation, the short-term stability is $\sigma_y(\tau) = (6,6 \pm 0.2) \times 10^{-10}\tau^{-0,50\pm0.1}$, showing an improvement of one order of magnitude

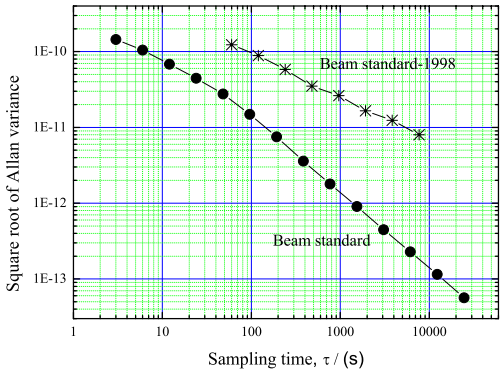

FIG. 7: Square root of the Allan deviation versus the sampling time.

IV. CONCLUSIONS

We presented a full evaluation of the operating Brazilian atomic standard. To evaluate some shifts and the Rabi frequency we have used a method well documented in the literature [7,11]. The evaluation of the frequency shifts is made directly from the experimental data. We analyzed the Ramsey pattern of the frequency standard to obtain the optimal Rabi frequency and the shift due to second-order Doppler effect. The biggest source of error in the standard is the quadratic Zeeman effect, influenced by the laboratory surroundings and indicating the necessity of a better magnetic shielding. The cavity pulling due to the oscillating field was also evaluated when the injected power was 2.5dB lower than the optimal value. The obtained shift was 1.27×10^{-13}. The Rabi pulling was also measured, and the obtained shift was 1.3×10^{-13} Hz. We have varied the C-field magnitude in order to assure that some inhomogeneity on the Ramsey fringes were due to these pullings. We noted that in the normal operation conditions there was a certain asymmetry in the most external fringes ($m_F = +3 \rightarrow m_F = +3$ and $m_F = -3 \rightarrow m_F = -3$). We suppose that it was due to Rabi and Ramsey pulling. The overal evaluation revels a short term stability of $6 \times 10^{-10}\tau^{-1/2}$, one order better than the beginning of our program.

We acknowledge the financial support obtained from FAPESP (CEPID/CEPOF), CAPES-COFECUB and Programa TIB-CNPq. We also acknowledge the important collaboration with BNM-SYRTE - Paris.

[1] Norman F. Ramsey, American Scientific, **76**, 42 (1988).
[2] Harold Lyons, Scientific American, **196**, 71 (1957).
[3] Norman F. Ramsey, Physics Today, p. 25, July 1980.
[4] F.Teles, D. V. Magalhães, M. S. Santos, G. D. Rovera, and V. S. Bagnato, IEEE, **47**, 1111 (2000).
[5] J. Vanier and C. Audoin, *" The Quantum Physics of Atomic Frequency Standard"*, Adam Hilger imprint by IOP Publishing LTD, 1989.
[6] A. Makdissi and E. de Clerq, IEEE Trans. Inst. Meas., **46**, 112 (1997).
[7] A Makdissi and E. de Clerq, Metrologia, **38**, 409 (2001).
[8] John H. Shirley, W. D. Lee, G. D. Rovera, and R. E. Drullinger, IEEE Trans. on Inst. and Meas., **44**, 136 (1995).
[9] E. Simon, P. Laurent, and A. Clairon, Phys. Rev. A, **57**, 436 (1998).
[10] J. H. Shirley, W. D. Lee, and R. E. Drullinger, Metrologia, **38**, 427 (2001).
[11] F.Teles, M. S. Santos, D. V. Magalhães, A. Bebeachibuli, and V. S. Bagnato, Metrologia, **39**, 135 (2002).